
Data report: permeability of ~1.9 km deep coal-bearing formation samples off the Shimokita Peninsula, Japan¹

Akira Ijiri,^{2,3} Yojiro Ikegawa,⁴ and Fumio Inagaki^{2,3,5}

Chapter contents

Abstract	1
Introduction	1
Methods and materials	2
Results	3
Acknowledgments	3
References	3
Figures	5
Tables	7

Abstract

We report the permeability of ~1.9 km deep coal-bearing formation samples retrieved at Site C0020 during Integrated Ocean Drilling Program Expedition 337 off the Shimokita Peninsula, Japan. The flow-through permeability test was conducted by a tri-axial consolidation permeability test device. The intrinsic permeability of lignite coal samples is $3.80 \times 10^{-20} \text{ m}^2$ and $3.61 \times 10^{-20} \text{ m}^2$ at 1919.57 and 1922.95 meters below seafloor (mbsf), respectively. In contrast, a sample from a sand layer interbedded with the coal layer at 1925.38 mbsf is unconsolidated and too soft to conduct permeability tests. The sand size fraction ($>75 \mu\text{m}$) is 88.5 wt%, and the estimated porosity is 40.5%.

Introduction

One of the scientific objectives of Integrated Ocean Drilling Program (IODP) Expedition 337 was to examine the feasibility of geological CO₂ sequestration in deep offshore coal-formation repositories (Inagaki et al., 2012). Riser drilling during Expedition 337 penetrated a 2466 m deep sedimentary sequence at Site C0020 that included a series of coal-bearing layers at ~1.9–2.0 km below seafloor where microbial methanogenesis via CO₂ reduction was observed (Inagaki et al., 2015). Hydrocarbon reservoirs (e.g., unmineable subsurface petroleum fields and coal beds) have been considered for use as geologic CO₂ repositories. Likewise, recovery of coal bed methane associated with hydrocarbon reservoirs is possibly facilitated by CO₂ injection and thus can contribute to decreasing the energy cost associated with such a venture (e.g., Gunter et al., 1997; White et al., 2003). To evaluate the potential of these applications, permeability data are important; however, permeability data from deeply buried offshore coal-bearing formations are rare. Here, we report relevant characteristics at Site C0020 by conducting flow-through permeability experiments on coal samples and grain-size analysis of a sand layer interbedded with the lignite coal.

¹Ijiri, A., Ikegawa, Y., and Inagaki, F., 2017. Data report: permeability of ~1.9 km-deep coal-bearing formation samples off the Shimokita Peninsula, Japan. *In* Inagaki, F., Hinrichs, K.-U., Kubo, Y., and the Expedition 337 Scientists, *Proceedings of the Integrated Ocean Drilling Program, 337*: Tokyo (Integrated Ocean Drilling Program Management International, Inc.).
doi:10.2204/iodp.proc.337.202.2017

²Kochi Institute for Core Sample Research, Japan Agency for Marine Science and Technology (JAMSTEC), Nankoku, Kochi 783-8502, Japan.
ijiri@jamstec.go.jp

³Research and Development Center for Submarine Resources, JAMSTEC, Yokosuka 237-0061, Japan.

⁴Civil Engineering Research Laboratory, Central Research Institute of Electric Power Industry (CRIEPI), Chiba 270-1194, Japan.

⁵Research and Development Center for Ocean Drilling Science, JAMSTEC, Yokohama 236-0001, Japan.



Methods and materials

Coal-bearing formation samples

We conducted permeability experiments on two lignite coal samples taken at 1919.57 and 1922.95 meters below seafloor (mbsf) and a grain-size analysis porosity measurement on one sand sample taken at 1925.38 mbsf from lithologic Unit III (1826.5–2046.5 mbsf) in a coal-bearing formation dominated by several coal horizons at Site C0020 (Inagaki et al., 2012). Water content, color, and vitrinite reflectance measurements suggest the coal has low maturity (Inagaki et al., 2012; Gross et al., 2015; Tanikawa et al., 2016). The sand sample is unconsolidated and extremely soft (i.e., beach sand) (see the “Site C0020” chapter [Expedition 337 Scientists, 2013]). The sand layers, which were almost impossible to retrieve intact by riserless drilling, were successfully recovered by riser drilling using high-density mud (Inagaki et al., 2012). Half-round core samples that yielded the coal samples were sealed by a gas barrier film (Escal Neo; Mitsubishi Gas Chemical Company, Inc., Japan) after collection and stored at 4°C to maintain their natural water content until sampling.

Permeability measurements

Permeability experiments were conducted on two cylindrical samples of coal retrieved from 1919.57 and 1922.95 mbsf (Table T1). Samples were taken directly from the sealed core and trimmed parallel to the core axis to allow assessment of vertical permeability. The sample from 1919.57 mbsf is 2.01 cm long and 1.6 cm in diameter, and the sample from 1922.95 mbsf is 1.80 cm long and 1.5 cm in diameter. Each specimen was placed in impermeable, flexible heat-shrink tubing and then loaded into a pressure vessel. The pressure vessel is connected to three pumps (Figure F1; Ohtomo et al., 2013). One pump controlled the pressure at the top of the specimen, one pump controlled the pressure at the bottom of the specimen, and one pump controlled the isostatic confining pressure around the specimen. Deionized water was used as the confining fluid and the permeant.

After the backpressure and confining pressure reached at 30 and 40 MPa, respectively, flow-through permeability tests were conducted by imposing a steady pressure gradient across the specimen while maintaining the isostatic effective stress at the center of the specimen. We didn’t conduct the backpressure saturation or consolidation of specimen before the tests.

Experimental conditions were selected to be similar to the in situ condition at the depth where the sample was collected. Confining pressure represents the total overburden above a specified depth. The total overburden was estimated as follows:

$$W = \rho_w \times d_w + \rho_b \times d_s, \quad (1)$$

where

W = total weight,

ρ_w = density of water,

d_w = water depth,

ρ_b = bulk density of sediment in water to consider buoyancy, and

d_s = sediment depth.

Considering the water depth at Site C0020 (1180 m), the density of seawater (1.02 g/cm³), the sediment depth where the sample was collected (~1900 mbsf), and the bulk density of the sediments from Site C0020 ranging from 1.7 to 2.3 g/cm³ (see the “Site C0020” chapter [Expedition 337 Scientists, 2013]), the total overburden in situ is estimated to be 44.3–55.7 MPa. Thus, we conducted the experiment at 40 and 50 MPa confining pressure with effective stress of 10 and 20 MPa, respectively, as similar conditions to the in situ pressure for the coal-bearing formation. After the experiments at 40 MPa, we increased the confining pressure to 50 MPa. The backpressure of 30 MPa was selected to be similar to the hydrostatic pressure at the specified depth (~3000 meters below sea level [mbsl]; ~30.6 MPa).

The temperature of the confining fluid was fixed at 50°C, which is similar to the ambient temperature at ~1900 mbsf (Inagaki et al., 2012; Tanikawa et al., 2016). The temperature of the confining fluid in the pressure vessel was regulated by a constant-temperature fluid circulating in which a silicon oil is circulated through the heater (Julabo, Baden-Württemberg, Germany, HE) and around the pressure vessel (Figure F1). The in situ temperature during the experiment is monitored by a thermocouple sensor attached to stoppers of the column.

All experiments were run after a steady state was achieved in which inflow and outflow volumes were equal while the sample length and pressure gradient remained constant. From the steady-state flow rate, sample dimensions, and pressure difference across the specimen, intrinsic permeability was calculated by rearranging Darcy’s law:

$$k = -Q\mu/A \times \Delta l/\Delta P, \quad (2)$$

where

- k = permeability,
- Q = steady-state flow rate,
- μ = fluid viscosity,
- A = cross-sectional area of the specimen,
- Δl = length of the specimen, and
- ΔP = fixed pressure difference across the specimen.

Fluid viscosity (μ) was referred to a physical table to adjust for temperature, which was measured nearly continuously during the experiments.

Grain-size distribution and porosity of sandy sediment

We analyzed the grain-size distribution and porosity in the sand sample from 1925.38 mbsf because the sample was too soft to conduct a permeability test (Table T1). The sand sample is unconsolidated beach sand (see the “Site C0020” chapter [Expedition 337 Scientists, 2013]), which is not sandstone at all and would be disturbed. It was impossible to trim the sample in a cylindrical form for the permeability test. Furthermore, the large flow rate is beyond the capacity of the cylinder pump equipped with our instrument was anticipated, even with a small pressure gradient across the specimen.

The porosity of the sand sample was estimated by gravimetric measurements. The sample was carefully placed into a cylindrical plastic chamber of known volume (1.7 cm³) by a spatula. Assuming that the sample was saturated by water, its saturated unit weight was estimated by weighing. The sample was then dried at 60°C and weighed again. The pore volume was estimated from the difference in weight between the wet and dry sample and the density of water. We used the density of pure water (1.0 g/cm³) for the estimation because the coal-bearing formation would be saturated by low-chlorinity water or freshwater and the absolute salt content was unknown (see the “Site C0020” chapter [Expedition 337 Scientists, 2013]). Porosity e was then estimated as follows:

$$e = V_v/V, \quad (3)$$

where

- V_v = pore volume and
- V = total sample volume.

For the measurement of grain-size distribution, the sample (~30 cm³) was dried at 60°C and the grain-size distribution was then determined by wet sieving at successive mesh sizes of 75, 90, 125, 150, 180, 250, 425, and 700 μm , followed by drying at 60°C for 3 days and weighing. The gradient of weight difference divided by dry time was checked to be small enough.

Results

The permeability determinations are listed in Table T2. Coefficients of permeability for the two coal samples are 1.31×10^{-9} cm/s and 1.23×10^{-9} cm/s at 40 MPa confining pressure and 6.72×10^{-11} cm/s and 6.38×10^{-11} cm/s at 50 MPa confining pressure, respectively. The intrinsic permeabilities of the two samples were 7.38×10^{-19} m² and 6.93×10^{-19} m² at 40 MPa confining pressure and 3.80×10^{-20} m² and 3.61×10^{-20} m² at 50 MPa confining pressure, respectively.

The results of the grain-size measurements are shown in Figure F2 and Table T3. The sand size fraction (passing through sieves coarser than 75 μm) is 88.5 wt%, and the silt and clay size fraction (<75 μm) is 11.5 wt%. The estimated porosity was 40.5%. For comparison, the estimated porosity is plotted with onboard measurements of core samples in Figure F3.

Acknowledgments

We thank the captains, crew members, and laboratory technicians of the *D/V Chikyu* for core recovery and sample collection. Samples were provided by the Integrated Ocean Drilling Program (IODP). This study was supported in part by the Japan Society for the Promotion of Science (JSPS) Strategic Fund for Strengthening Leading-Edge Research and Development (to JAMSTEC and F. Inagaki), the JSPS Funding Program for Next Generation World-Leading Researchers (NEXT Program, GR102 to F. Inagaki), and Grants-in-Aid for Science Research (No. 26287128 to A. Ijiri; No. 26251041 to F. Inagaki). The authors are grateful to A. Imajyo for technical assistance. We acknowledge our anonymous reviewers for their contribution to improving the report.

References

- Expedition 337 Scientists, 2013. Expedition 337 Site C0020. In Inagaki, F., Hinrichs, K.-U., Kubo, Y., and the Expedition 337 Scientists, *Proceedings of the Integrated Ocean Drilling Program, 337*: Tokyo (Integrated Ocean Drilling Program Management International, Inc.). <https://doi.org/10.2204/iodp.proc.337.103.2013>
- Gross, D., Bechtel, A., and Harrington, G.J., 2015. Variability in coal facies as reflected by organic petrological and geochemical data in Cenozoic coal beds offshore Shimokita (Japan)—IODP Exp. 337. *International Journal of Coal Geology*, 152(B):3–79. <https://doi.org/10.1016/j.coal.2015.10.007>
- Gunter, W.D., Gentzis, T., Rottenfusser, B.A., and Richardson, R.J.H., 1997. Deep coalbed methane in Alberta, Canada: a fuel resource with the potential of zero green-

- house gas emissions. *Energy Conversion and Management*, 38(Suppl.):S217–S222. [https://doi.org/10.1016/S0196-8904\(96\)00272-5](https://doi.org/10.1016/S0196-8904(96)00272-5)
- Inagaki, F., Hinrichs, K.-U., Kubo, Y., and the Expedition 337 Scientists, 2012. Deep coalbed biosphere off Shimokita: microbial processes and hydrocarbon system associated with deeply buried coalbed in the ocean. *Integrated Ocean Drilling Program Preliminary Report*, 337. <https://doi.org/10.2204/iodp.pr.337.2012>
- Inagaki, F., Hinrichs, K.-U., Kubo, Y., Bowles, M.W., Heuer, V.B., Long, W.-L., Hoshino, T., Ijiri, A., Imachi, H., Ito, M., Kaneko, M., Lever, M.A., Lin, Y.-S., Methé, B.A., Morita, S., Morono, Y., Tanikawa, W., Bihan, M., Bowden, S.A., Elvert, M., Glombitza, C., Gross, D., Harrington, G.J., Hori, T., Li, K., Limmer, D., Liu, C.-H., Murayama, M., Ohkouchi, N., Ono, S., Park, Y.-S., Phillips, S.C., Prieto-Mollar, X., Purkey, M., Riedinger, N., Sanada, Y., Sauvage, J., Snyder, G., Susilawati, R., Takano, Y., Tasumi, E., Terada, T., Tomaru, H., Trembath-Reichert, E., Wang, D.T., and Yamada, Y., 2015. Exploring deep microbial life in coal-bearing sediment down to ~2.5 km below the ocean floor. *Science*, 349(6246):420–424. <https://doi.org/10.1126/science.aaa6882>
- Ohtomo, Y., Ijiri, A., Ikegawa, Y., Tsutsumi, M., Imachi, H., Uramoto, G.-I., Hoshino, T., Morono, Y., Sakai, S., Saito, Y., Tanikawa, W., Hirose, T., and Inagaki, F., 2013. Biological CO₂ conversion to acetate in subsurface coal-sand formation using a high-pressure reactor system. *Frontiers in Microbiology*, 4:361. <https://doi.org/10.3389/fmicb.2013.00361>
- Tanikawa, W., Tadai, O., Morita, S., Lin, W., Yamada, Y., Sanada, Y., Moe, K., Kubo, Y., and Inagaki, F., 2016. Thermal properties and thermal structure in the deep-water coalbed basin off the Shimokita Peninsula, Japan. *Marine and Petroleum Geology*, 73:445–461. <https://doi.org/10.1016/j.marpetgeo.2016.03.006>
- White, D.J., Burrowes, G., Davis, T., Hajnal, Z., Hirsche, K., Hutcheon, I., Majer, E., Rostron, B., and Whittaker, S., 2003. Greenhouse gas sequestration in abandoned oil reservoirs: the International Energy Agency Weyburn pilot project. *GSA Today*, 14(7):4–10. [https://doi.org/10.1130/1052-5173\(2004\)014<004:GGSIAO>2.0.CO;2](https://doi.org/10.1130/1052-5173(2004)014<004:GGSIAO>2.0.CO;2)
- Initial receipt:** 12 April 2016
Acceptance: 2 May 2017
Publication: 7 July 2017
MS 337-202

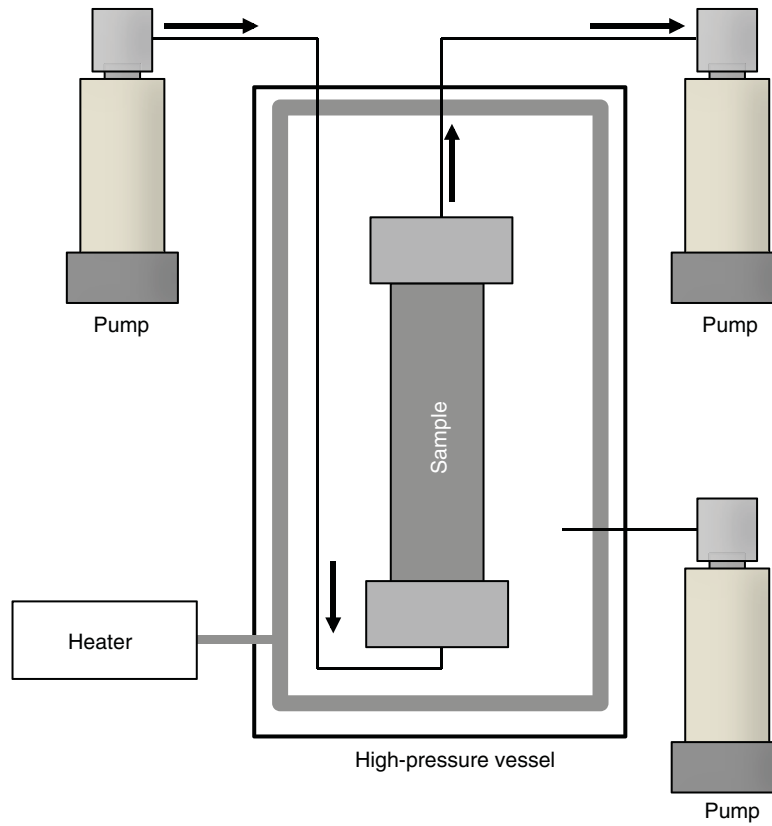
Figure F1. Triaxial consolidation permeability test device.

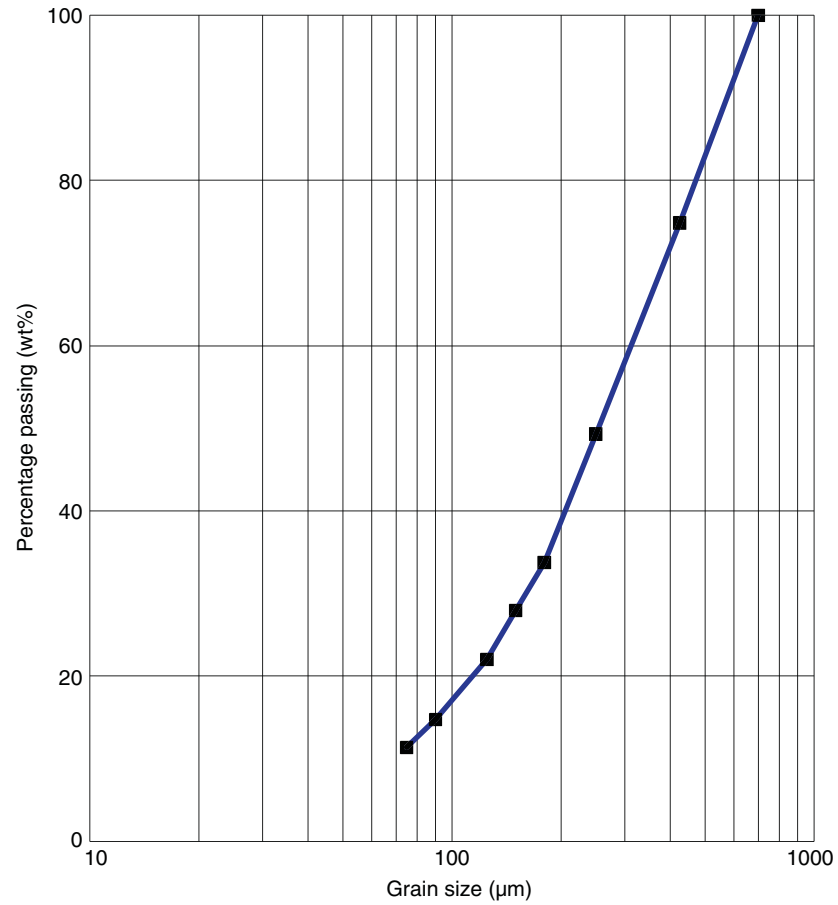
Figure F2. Grain-size distribution of sand sample from 1925.38 mbsf, Hole C0020A.

Figure F3. Porosity of sand sample from 1925.38 mbsf, Hole C0020A. Distribution and lithologic variation of porosity in discrete core samples measured onboard are also shown (see the “Site C0020” chapter [Expedition 337 Scientists, 2013]).

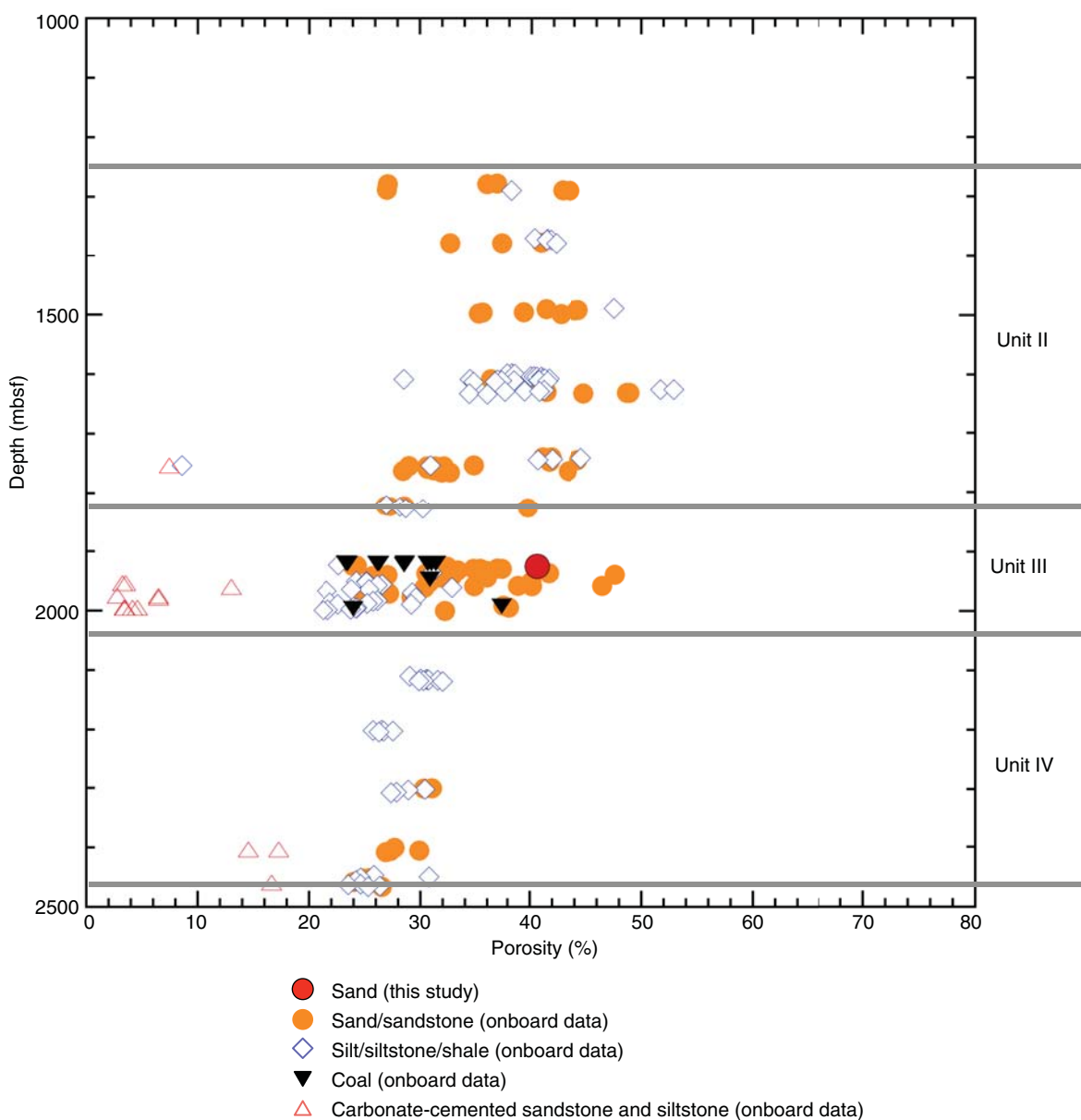


Table T1. Permeability and grain-size test samples, Hole C0020A.

Core, section, interval (cm)	Depth (mbsf)	Test	Lithology
337-C0020A-			
15R-1, 56–59	1919.57	Permeability	Coal
15R-4, 72.5–75.5	1922.95	Permeability	Coal
15R-6, 130–134	1925.38	Grain size	Sand

Table T2. Permeability test results, Hole C0020A.

Measurement	Unit	337-C0020A-15R-1, 56-59 cm		337-C0020A-15R-4, 72.5-75.5 cm	
Confining pressure	MPa	40	50	40	50
Time	h	2.17	14.64	2.47	14.53
Volume change	cm ³	0.20077322	0.06974	0.20154762	0.07035255
Volumetric flow rate	cm ³ /h	0.092545914	0.004762215	0.093021978	0.004842623
Pressure difference	Mpa	0.5	0.5	0.5	0.5
Difference of water head	cm	4901.96	4901.96	4901.96	4901.96
Length of the specimen	cm	2.01	2.01	1.80	1.80
Area of the specimen	cm ²	32.31	32.31	30.96	30.96
Hydraulic gradient	‰	2438.79	2438.79	2723.31	2723.31
Flow velocity	cm/h	2.86E-03	1.47E-04	3.00E-03	1.56E-04
Coefficient of permeability	cm/h	1.17E-06	6.04E-08	1.10E-06	5.74E-08
	cm/s	3.26E-10	1.68E-11	3.06E-10	1.60E-11
Intrinsic permeability	m ²	3.20E-17	1.68E-18	3.06E-17	1.60E-18

Table T3. Grain-size measurements, Hole C0020A.

Sieve size (μm)	Passing weight (g)	Passing percent (%)	Cumulative percent (%)
700			100
425	5.77	25.1	74.9
250	5.86	25.5	49.3
180	3.58	15.6	33.8
150	1.34	5.8	27.9
125	1.35	5.9	22.0
90	1.68	7.3	14.7
75	0.76	3.3	11.4
Pan	2.62	11.4	0.0